NASA TECHNICAL NOTE

NASA TN D-3034

NASA TN D-3034

EFFECTS OF THICKNESS ON SUPERSONIC PERFORMANCE OF A WING-BODY CONFIGURATION EMPLOYING A WARPED HIGHLY SWEPT ARROW WING

by F. Edward McLean and Dennis E. Fuller

Langley Research Center
Langley Station, Hampton, Va.

NATIONAL AERONAUTICS AND SPACE ADMINISTRATION • WASHINGTON, D. C. • OCTOBER 1965

NASA TN D-3034

EFFECTS OF THICKNESS ON SUPERSONIC PERFORMANCE OF A WING-BODY CONFIGURATION EMPLOYING A WARPED HIGHLY SWEPT ARROW WING

By F. Edward McLean and Dennis E. Fuller

Langley Research Center
Langley Station, Hampton, Va.

NATIONAL AERONAUTICS AND SPACE ADMINISTRATION

For sale by the Clearinghouse for Federal Scientific and Technical Information
Springfield, Virginia 22151 – Price $2.00

EFFECTS OF THICKNESS ON SUPERSONIC PERFORMANCE OF A WING-BODY CONFIGURATION EMPLOYING A WARPED HIGHLY SWEPT ARROW WING

By F. Edward McLean and Dennis E. Fuller
Langley Research Center

SUMMARY

An investigation has been conducted to determine some effects of airfoil-section shape and thickness on the performance of a wing-body configuration which employed a warped highly swept arrow wing. The wing planform had 76° leading-edge sweep, and aspect ratio of 1.71, and the wing tips were clipped perpendicular to the stream direction. The warped mean surface of the wing was designed for a Mach number of 2.6 and the lift coefficient (0.063) was purposely limited to a value well below the theoretical optimum lift coefficient of 0.148. Airfoil-section shapes and thickness distributions applied to the basic mean surface were streamwise $2\frac{1}{2}$-percent-thick circular-arc, 4-percent-thick circular-arc, and $2\frac{1}{2}$-percent-thick NACA 65-series sections, respectively. For the $2\frac{1}{2}$-percent-thick circular-arc and NACA 65-series thickness distributions flat reference models were tested for comparison. The body of the configuration was scaled to satisfy volume and space requirements of a supersonic transport.

Wind-tunnel tests of the various models of the wing-body configuration were conducted at Mach numbers of 2.4, 2.6, and 2.86 and at a Reynolds number (based on the wing mean aerodynamic chord) of 3.5×10^6. At a Mach number of 2.6 for the particular combinations of wing parameters considered, the results indicated that increased wing thickness had a degrading effect on the drag-due-to-lift performance of the basic warped lifting surface. For the same thickness ratio, the sharp leading-edge circular-arc thickness distribution provided better aerodynamic performance than the rounded leading-edge NACA 65-series section at Mach numbers of 2.6 and 2.86. At a Mach number of 2.4, which is below the design Mach number of 2.6, use of the 65-series thickness distribution on the warped wing surface resulted in a slightly better performance. For the airfoil shapes and thickness distributions of the tests, the warped lifting surface was responsible for longitudinal trim advantages and aerodynamic performance gains over reference flat lifting surfaces. These gains, however, were below theoretical estimates.

INTRODUCTION

A number of theoretical papers (refs. 1 to 3, for example) have indicated the supersonic performance advantages which should accrue from the use of the optimum twist and camber or wing-warp concepts of linearized theory and have pointed out the classes of wing planform for which these concepts are theoretically applicable (ref. 4). However, since the several attempts to verify the theoretical potential of the optimum wing concepts have met with little success (refs. 4 and 5), alternate approaches to the supersonic wing design problem have been suggested (ref. 6). The current interest in the development of an efficient supersonic transport has led to further consideration of the most promising of these approaches.

The supersonic wing design procedure considered herein was suggested by the results of references 6 and 7. This research indicated that, under real flow conditions, a desired wing lift can be produced more efficiently by a design-lift-limited warped surface at an angle of attack than by either a flat lifting surface or by a linearized theory optimum surface designed to produce the entire lift. Thus, it could be inferred that past failures with the optimum concepts of theory were caused partially by the severity of the lift requirement imposed in the wing design. With a limitation on the overall magnitude of the design lift coefficient, and a subsequent limitation on the severity of the wing surface distortion, desirable performance advantages over a corresponding flat wing were realized (refs. 6 and 7). The primary purpose of the present investigation was to determine some of the effects of airfoil-section shape and thickness on the performance of a wing-body configuration which utilizes a warped wing with a relatively low design lift coefficient as compared with the optimum. The secondary purpose was to explore the design-lift-limited warped surface concept at more extreme Mach number and planform conditions than those considered by the research of references 6 and 7.

Five wing-body models were constructed for the present investigation. Each of the models had the same clipped arrow wing planform with 76° leading-edge sweep and an aspect ratio of 1.71. The body of each model had the same longitudinal area distribution and was scaled to satisfy the volume and space requirements of a supersonic transport. The warped mean wing surface of the three models was designed for a Mach number of 2.6 and the design lift coefficient (0.063) was purposely limited to a value well below the theoretical optimum lift coefficient of 0.148. Streamwise $2\frac{1}{2}$-percent-thick circular-arc, 4-percent-thick circular-arc, and $2\frac{1}{2}$-percent-thick NACA 65-series thickness distributions, respectively, were added symmetrically to the common warped surface to determine thickness effects. The other two models were reference models which employed a flat lifting surface with $2\frac{1}{2}$-percent-thick circular-arc, and $2\frac{1}{2}$-percent-thick NACA 65-series sections, respectively.

The five models of the wing-body configuration were tested in the Langley Unitary Plan wind tunnel at Mach numbers of 2.4, 2.6, and 2.86 at a Reynolds number (based on the wing mean aerodynamic chord) of 3.5×10^6. Lift, drag,

and longitudinal stability characteristics are presented along with some comparisons with theory.

SYMBOLS

The results are referred to the stability-axis system with the moment reference center located at a station corresponding to the quarter-chord point of the mean aerodynamic chord as shown in figure 1. The coefficients and symbols are defined as follows:

b wing span, 20 inches

$\bar{c}$ wing mean aerodynamic chord, 13.97 inches

C_D drag coefficient, $\frac{\text{Drag}}{qS}$

$C_{D,0}$ drag coefficient at zero lift

$C'_{D,0}$ drag coefficient of flat reference model at zero lift

C_L lift coefficient, $\frac{\text{Lift}}{qS}$

C_m pitching-moment coefficient, $\frac{\text{Pitching moment}}{qS\bar{c}}$

H, R_1, R_2, R_3, z_b coordinates of body cross sections (See table II.)

L/D lift-drag ratio

M free-stream Mach number

$m = \cot \Lambda$

q free-stream dynamic pressure, lb/sq ft

$r = \frac{y}{mx'}$

S wing planform area, 1.62 sq ft

x,y,z	distance along the X-, Y-, and Z-axis, respectively
x'	streamwise distance measured from wing apex, inches (table I)
z_c	wing mean camber surface ordinate, inches (table I)
α	angle of attack, degree
Λ	leading-edge sweep angle (76°)

APPARATUS AND METHODS

Wind Tunnel

The tests were conducted in the low Mach number test section of the Langley Unitary Plan wind tunnel, which is a variable pressure, continuous return flow tunnel. The test section is 4 feet square and approximately 7 feet long. The tunnel is equipped with a central support system which permits remote control of the angle of attack of a sting-mounted model.

Models and Instrumentation

Five wing-body models of a selected wing-body configuration were considered in the present investigation. Two classes of lifting surface were considered, flat and warped. Similarly, two types of airfoil section were considered - the sharp leading-edge circular-arc section and the rounded-leading-edge (leading-edge radius = 0.000425 chord) NACA 65-series section. The following table gives the model designations and some wing variables:

Model	Lifting-surface design condition	Streamwise thickness distribution	Model designation
1	Flat, design $C_L = 0$	$2\frac{1}{2}$-percent circular-arc	Flat CA-025
2	Warped, design $C_L = 0.063$	$2\frac{1}{2}$-percent circular-arc	Warped CA-025
3	Warped, design $C_L = 0.063$	4-percent circular-arc	Warped CA-040
4	Flat, design $C_L = 0$	$2\frac{1}{2}$-percent NACA 65-series	Flat 65-025
5	Warped, design $C_L = 0.063$	$2\frac{1}{2}$-percent NACA 65-series	Warped 65-025

The wing planform, which is the same for all models, was selected on the basis of the linearized theory that, at supersonic speeds, lift may be produced most efficiently by an arrow wing which has subsonic leading edges and highly swept trailing edges (ref. 4). The wing had 76° leading-edge sweep, an aspect ratio of 1.71, and the wing tips were clipped perpendicular to the stream direction. A representative layout of the flat reference models 1 and 4 is shown in figure 1(a), and a representative layout of the warped-lifting-surface models 2, 3, and 5 is shown in figure 1(b).

The lift-limited warped lifting surface which was utilized by models 2, 3, and 5 was designed for a Mach number of 2.6 and a lift coefficient of 0.063 according to the concepts and methods discussed in the section on design considerations. The original calculated mean lifting surface was sheared, as indicated in figure 2, to provide a more acceptable surface for the possible installation of a variable-sweep mechanism. Within the linear-theory concepts used, this vertical shearing should not affect the anticipated results. The final mean camber surface ordinates are presented in table I.

The bodies, which had the same longitudinal cross-sectional-area development for each model, were scaled to represent the volume and space requirements of a supersonic transport. The body ordinates in inches are presented in table II. The body and wing of each model was oriented so that the body volume was equally distributed above and below the mean camber surface of the wing.

The models, which were cast of no. 225 gun metal bronze, were sting mounted from the tunnel central support system, and the forces and moments were obtained on a six-component strain-gage balance mounted within the model.

Tests

The wind-tunnel tests were conducted at the following conditions:

Mach number	2.40	2.60	2.86
Reynolds number (based on $\bar{c}$) . .	3.5×10^6	3.5×10^6	3.5×10^6
Stagnation pressure, lb/sq ft . .	2405	2680	3075
Stagnation pressure, ^{o}F	150	150	150
Dewpoint, ^{o}F	-30	-30	-30

The basic aerodynamic characteristics of the five models were obtained with a 1/16-inch-wide strip of no. 60 grit carborundum located 15/16 inch from the body nose and with 1/16-inch-wide transition strips of no. 120 grit carborundum located 1/16 inch and perpendicular to the wing leading edges.

Corrections and Accuracy

The maximum deviation of local Mach number in the part of the tunnel occupied by the models is ±0.015 from the average value given. The average angularity of the flow in the region of the models was determined by comparing inverted and upright tests, the angle of attack being corrected accordingly. The angles of attack have been corrected for balance and sting deflection and are accurate to within $\pm 0.1^{o}$. The data has been adjusted to the condition of free-stream static pressure at the model chamber.

Based upon balance accuracy and repeatability of data, it is estimated that the measured quantities are accurate within the following limits:

C_L	±0.003
C_D	±0.0005
C_m	±0.0005

Design Considerations

The general concept of the optimum supersonic wing design methods of linearized theory is that these methods allow the attainment of lift distributions over a given subsonic-edge wing planform which are favorable but do not have to fulfill the flat-plate requirement of infinite negative pressures near the leading edge. However, in reference 6, the finite-pressure methods call for extreme leading-edge pressures and extreme surface distortions in the optimum design lift coefficient range of most supersonic configurations. Thus, the magnitude of the design lift requirement necessary to maintain finite leading-edge pressures at near optimum conditions is generally sufficient to violate linearized theory as to the lifting-surface geometry and local flow conditions.

References 6 and 7 indicated that, under real flow conditions, a limitation of the design lift coefficient and the subsequent acceptance of infinite leading-edge pressure resulted in a better approximation to linearized theory than the optimum finite-pressure methods.

Since the limited-design-lift-coefficient concept appeared to merit further consideration, the drag-interference terms between the flat-plate loading and the truncated orthogonal loadings developed in references 3 and 8 were calculated for a number of highly swept clipped arrow-wing planforms. On the basis of these calculations, the wing planform described in the section "Models and Instrumentation" was selected for the present investigation. For the planform and design Mach number (2.6) selected, the expression for the drag coefficient of the wing-body configuration is

$$C_D = C'_{D,0} + 0.346\left(C_{L,\text{design}}\right)^2 - 0.685C_L\left(C_{L,\text{design}}\right) + 0.6694C_L^2 \qquad (1)$$

With a $C'_{D,0}$ of 0.0072 estimated for the wing-body configuration, equation (1) can be used to show that, for the test conditions selected, optimum considerations would require a highly warped-surface design lift coefficient of 0.148 with a theoretical maximum L/D potential of 10.2. However, with the chosen lift-limited design lift coefficient of 0.063, the wing surface would be much less severely warped but a relatively high theoretical maximum L/D potential of 9.2 would remain. The flat reference models 1 and 4 would have a theoretical maximum L/D potential of 7.2. It should be pointed out that design lift coefficient strongly influences the self-trimming characteristics of a warped surface and from this standpoint the chosen design lift coefficient is lower than required. However, the main purpose of the present investigation was to consider thickness effects which would have little influence on trim characteristics at the design Mach number.

RESULTS AND DISCUSSION

Basic Aerodynamic Characteristics

Wind-tunnel tests of the five basic wing-body configurations discussed in preceding sections have been conducted in the Langley Unitary Plan wind tunnel. The measured aerodynamic characteristics in pitch of the three wing-body models which employed circular-arc thickness distributions are presented in figure 3. For ease in making comparisons, the data for the three Mach numbers are included in the same figure.

The results shown in figure 3, as would be expected, indicate a relatively small effect of thickness on the lift characteristics (fig. 3(a)) and pitching-moment coefficients (fig. 3(b)) of the wing-body configuration. The primary effect of wing warp (model 2 and model 3) was to reduce the angle of attack required for a given lift compared with that of the flat-wing model (model 1). A more important characteristic of wing warping was the indicated reduction in the pitching moment required to trim the configuration. This effect is one of the most important reasons for the consideration of wing warp in the design of supersonic airplanes.

It is shown in figures 3(c) and 3(d) that the wing body with limited warped surface and $2\frac{1}{2}$-percent-thick circular-arc sections (model 2) had a better aerodynamic performance than the corresponding flat-wing model (model 1). Largely because of higher values of $C'_{D,0}$, the performance of model 3 with 4-percent-thick circular-arc section does not compare favorably with that of the thinner model (model 2). However, the thicker warped model (model 3) shows better performance than the flat reference model (model 1) except at the highest Mach number, 2.86.

The aerodynamic characteristics presented in figure 4 for the wing-body configuration with $2\frac{1}{2}$-percent-thick NACA 65-series airfoil sections indicate the same effects of warped surface on the lift and pitching-moment characteristics as those discussed in connection with the circular-arc sections. Similarly, use of the warped lifting surface in conjunction with the NACA 65-series sections (model 5) leads to increased aerodynamic performance over that obtained with the corresponding flat lifting surface (model 4).

A comparison of the aerodynamic efficiency (L/D) of the wing-body configuration with the warped lifting surface and the $2\frac{1}{2}$-percent-thick circular-arc and the $2\frac{1}{2}$-percent-thick NACA 65-series airfoil sections, respectively, is indicated in figure 5. This figure shows that the sharp-leading-edge circular-arc airfoil section provided a better performance than did the rounded-leading-edge 65-series section at the design Mach number of 2.6 and above the design Mach number at 2.86. Since model 2 had a higher zero-lift drag coefficient than model 5 (compare figs. 3(c) and 4(c)), this performance advantage can be attributed to the better lifting efficiency of the warped surface when the sharp leading-edge circular-arc sections are employed. Below the design Mach number

at $M = 2.4$, the performance of model 5 was slightly better principally because of an improvement in the relative lifting efficiency of the rounded leading-edge model (model 5) compared with the sharp leading-edge model (model 2).

Comparison of Experimental Results With Theory

Comparisons of the lift-drag ratios obtained experimentally at the design Mach number of 2.6 with those predicted by theory are presented in figure 6 for the three wing-body models which utilized the sharp leading-edge circular-arc airfoil sections. Similar comparisons for the two models which had the rounded-leading-edge NACA 65-series thickness distributions are shown in figure 7. In figures 6 and 7 for the wing-body and limited warped surface considered, the predicted increase in lifting efficiency is represented by the increment in lift-drag ratio between the theoretical curves for the flat plate without leading-edge suction and the theoretical curves for the warped surface.

It can be seen from figure 6 that the experimental results for the flat reference model (model 1) agree closely with the theoretical estimates for the flat plate without leading suction. The warped models with circular-arc sections (model 2 and model 3) are shown to provide some of the lifting-surface potential predicted by theory. Although the indicated potential is well below theoretical estimates, this gain, in combination with the trim advantages of the warped surface, is worthy of consideration in supersonic design. Since the thicker model (model 3) did not recover as much of the theoretical potential as did model 2, for the particular wing-body configurations investigated it would appear that increased thickness has a degrading effect on the lifting efficiency of a warped surface.

The comparisons of figure 7 for the wing-body models with NACA 65-series airfoil sections indicate trends similar to those discussed in connection with models 1 to 3. The flat reference model (model 4) agreed closely with the theoretical estimates for the flat plate without leading-edge suction, and the warped model (model 5) provided some of the lifting-surface potential predicted by theory. For similar thickness ratios, however, the warped surface with NACA 65-series airfoil sections did not provide as much aerodynamic potential at a Mach number of 2.6 as the warped surface with circular-arc sections. However, these results are for a particular combination of warped surface and rounded leading-edge airfoil section, and no general conclusions should be drawn.

CONCLUSIONS

An investigation has been made at a Mach number M of 2.4, 2.6, and 2.86 to determine some of the effects of section shape and thickness on the aerodynamic characteristics of a wing-body configuration employing a moderately warped highly swept arrow wing. For the particular choice of wing-design parameters used in the investigation, the results indicated the following conclusions:

1. At the design Mach number of 2.6 increased thickness had a degrading effect on the lifting efficiency of the warped surface.

2. A sharp leading-edge circular-arc airfoil section provided better lifting surface efficiency at the design Mach number than did a rounded-leading-edge (leading-edge radius = 0.000425 chord) NACA 65-series thickness distribution.

3. The circular-arc section provided better performance above the design Mach number at $M = 2.86$, whereas the NACA 65-series section provided slightly better performance below the design Mach number at $M = 2.4$.

4. For the section shapes and thickness distributions considered, the warped lifting surface was responsible for trim advantages and performance advantages over the corresponding flat reference configurations. The performance gains, however, were below theoretical estimates.

Langley Research Center,
National Aeronautics and Space Administration,
Langley Station, Hampton, Va., May 19, 1965.

REFERENCES

1. Ginzel, I.; and Multhopp, H.: Wings With Minimum Induced Drag in Supersonic Flow. Eng. Rept. No. 9937-M, The Glenn L. Martin Co., Aug. 1957.

2. Yoshihara, H.; Kainer, J.; and Strand, T.: On Optimum Thin Lifting Surfaces at Supersonic Speeds. J. Aero/Space Sci., vol. 25, no. 8, Aug. 1958, pp. 473-479, 496.

3. Grant, Frederick C.: The Proper Combination of Lift Loadings for Least Drag on a Supersonic Wing. NACA Rept. 1275, 1956. (Supersedes NACA TN 3533.)

4. Brown, Clinton E.; and McLean, Francis E.: The Problem of Obtaining High Lift-Drag Ratios at Supersonic Speeds. J. Aero/Space Sci., vol. 26, no. 5, May 1959, pp. 298-302.

5. Katzen, Elliott D.: Idealized Wings and Wing-Bodies at a Mach Number of 3. NACA TN 4361, 1958.

6. Brown, Clinton E.; McLean, F. E.; and Klunker, E. B.: Theoretical and Experimental Studies of Cambered and Twisted Wings Optimized for Flight at Supersonic Speeds. Advan. in Aeron. Sci., vol. 3, Pergamon Press, 1961, pp. 415-431.

7. Carlson, Harry W.: Aerodynamic Characteristics at Mach Number 2.05 of a Series of Highly Swept Arrow Wings Employing Various Degrees of Twist and Camber. NASA TM X-332, 1960.

8. Tucker, Warren A.: A Method for the Design of Sweptback Wings Warped To Produce Specified Flight Characteristics at Supersonic Speeds. NACA Rept. 1226, 1955. (Supersedes NACA RM L51F08.)

TABLE I.- CAMBER-SURFACE ORDINATES FOR MODELS 2, 3, AND 5

[Dimensions are in inches]

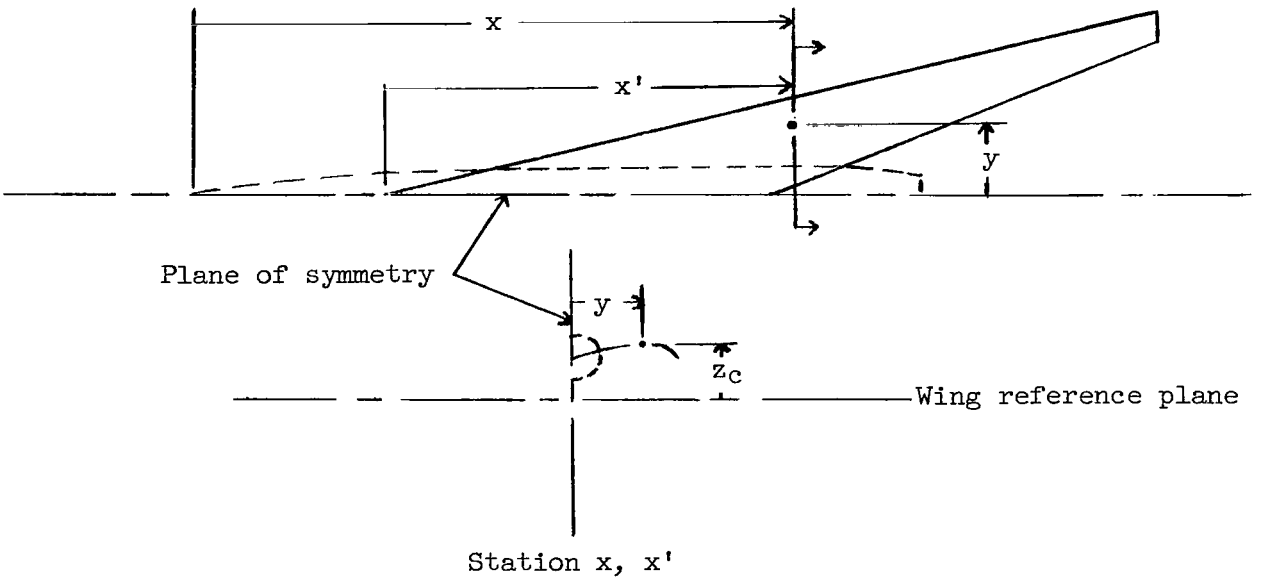

$r = \frac{y}{mx'}$	Camber-surface ordinate z_c at -						
	x = 10 x' = 0	x = 12 x' = 2	x = 14 x' = 4	x = 16 x' = 6	x = 18 x' = 8	x = 20 x' = 10	x = 22 x' = 12
0	1.0120	0.9220	0.7840	0.6480	0.5200	0.4200	0.3380
.0800		.9268	.7992	.6720	.5512	.4556	.3820
.1600		.9308	.8128	.6948	.5812	.4908	.4188
.2400		.9340	.8240	.7160	.6132	.5240	.4516
.3200		.9368	.8340	.7368	.6288	.5560	.4800
.4000		.9388	.8440	.7540	.6656	.5812	.5088
.4800		.9392	.8540	.7676	.6848	.6016	.5292
.6000		.9380	.8608	.7832	.7036	.6264	.5504
.7000		.9360	.8608	.7808	.7068	.6264	.5508
.8000		.9316	.8536	.7676	.6868	.6064	.5320
.8800		.9244	.8360	.7480	.6600	.5760	.4960
.9200		.9188	.8228	.7300	.6412	.5540	.4744
.9400		.9156	.8164	.7200	.6272	.5384	.4576
.9600		.9116	.8088	.7092	.6140	.5240	.4368
.9800		.9076	.8004	.6976	.5960	.5052	.4168
1.0000		.9016	.7884	.6784	.5744	.4736	.3840

TABLE I.- CAMBER-SURFACE ORDINATES FOR MODELS 2, 3, AND 5 - Concluded

$r = \frac{y}{mx'}$	Camber-surface ordinate z_c at -						
	x = 24 x' = 14	x = 26 x' = 16	x = 28 x' = 18	x = 30 x' = 20	x = 32 x' = 22	x = 34 x' = 24	x = 36 x' = 26
0	0.2680	0.2180	0.2020	0.1980	------	------	------
.0800	.3060	.2508	.2188	.2060	------	------	------
.1515	------	------	------	------	0.1600	------	------
.1600	.3384	.2808	.2356	.2192	.1720	------	------
.2400	.3712	.3080	.2552	.2216	.2016	------	------
.2778	------	------	------	------	------	0.1212	------
.3200	.3988	.3320	.2732	.2308	.2120	.1240	------
.3846	------	------	------	------	------	------	0.0876
.4000	.4248	.3568	.2884	.2384	.2120	.1280	.0852
.4800	.4472	.3780	.3040	.2500	.2120	.1368	.0864
.6000	.4748	.4040	.3312	.2600	.2120	.1436	.0928
.7000	.4812	.4096	.3412	.2760	.2120	.1540	.1200
.8000	.4616	.3912	.3280	.2740	.2120	.1860	.1880
.8800	.4232	.3556	.2864	.2360	.2120	.2240	.2400
.9200	.3948	.3240	.2560	.2120	.2120	.2280	.2440
.9400	.3980	.3048	.2376	.2000	.2080	.2240	.2400
.9600	.3592	.2812	.2160	.1860	.2000	.2160	.2280
.9800	.3332	.2540	.1920	.1680	.1740	.2000	.2040
1.0000	.2960	.2120	.1496	.1360	.1400	.1600	.1720

$r = \frac{y}{mx'}$	Camber-surface ordinate z_c at -						
	x = 38 x' = 28	x = 40 x' = 30	x = 42 x' = 32	x = 44 x' = 34	x = 46 x' = 36	x = 48 x' = 38	x = 50 x' = 40
0.4762	0.0560	------	------	------	------	------	------
.4800	.0552	------	------	------	------	------	------
.5200	.0432	------	------	------	------	------	------
.5555	------	0.0264	------	------	------	------	------
.6000	.0400	.0168	------	------	------	------	------
.6250	------	------	0.0080	------	------	------	------
.6500	.0520	.0348	.0300	------	------	------	------
.6863	------	------	------	0.0704	------	------	------
.7000	.0880	.0832	.0840	.0920	------	------	------
.7407	------	------	------	------	0.1560	------	------
.7500	.1520	.1528	.1580	.1640	.1680	------	------
.7895	------	------	------	------	------	0.2240	------
.8000	.2040	.2144	.2200	.2280	.2360	.2400	------
.8333	------	------	------	------	------	------	0.2760
.8400	.2320	.2452	.2520	.2600	.2680	.2760	.2840
.9200	.2560	.2720	.2840	.2960	.3040	.3160	.3240
.9400	.2520	.2680	.2800	.2920	.3040	.3120	.3240
.9600	.2440	.2560	.2680	.2800	.2920	.3000	.3080
.9800	.2240	.2360	.2480	.2600	.2720	.2760	.2880
1.0000	.1800	.1920	.2000	.2080	.2160	.2240	.2320

TABLE II.- BODY CROSS SECTIONS OF TEST MODELS

[Dimensions are in inches]

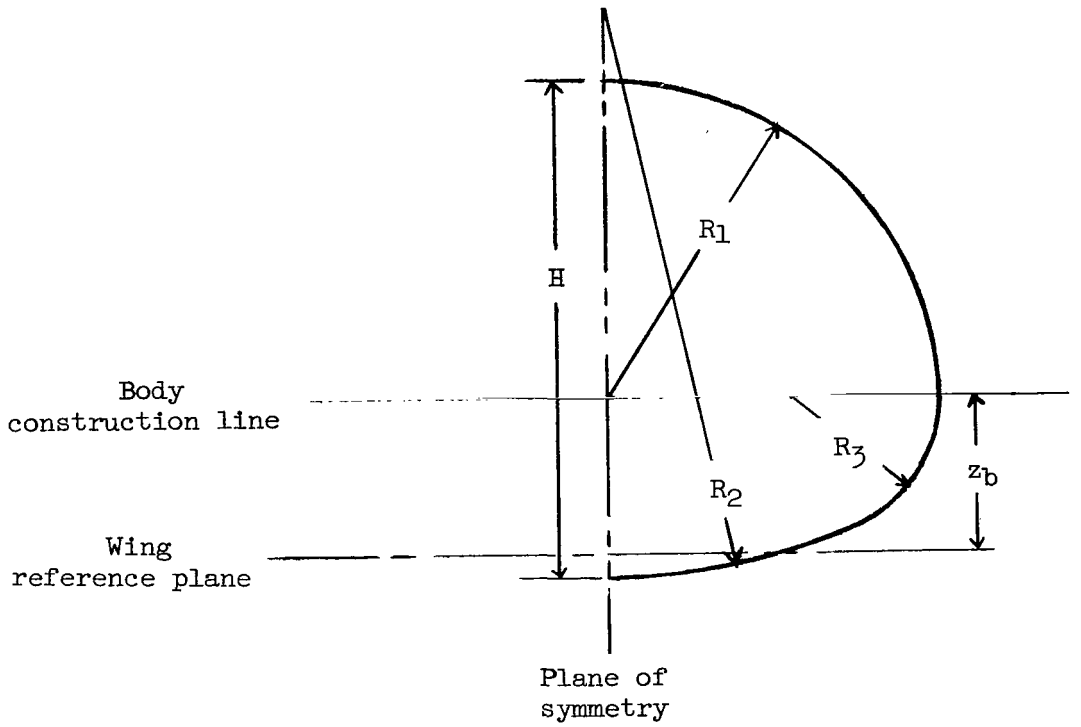

Model station, x	R_1	R_2	R_3	H	z_b for models 1 and 4	z_b for models 2, 3, and 5
0	0	0	0	0	0	1.218
2	.3300	.6640	.2090	.5560	-.051	1.129
4	.6100	1.2260	.3860	1.0260	-.108	1.044
6	.8500	1.7070	.5370	1.4290	-.156	.966
8	1.0600	2.1290	.6700	1.7820	-.181	.889
10	1.2100	2.4300	.7650	2.0340	-.192	.820
12	1.3200	2.6520	.8350	2.2200	-.199	.723
14	1.3800	2.7700	.8720	2.3190	-.198	.586
16	1.4005	2.8116	.8850	2.3543	-.198	.450
18	↓	↓	↓	↓	-.186	.334
20					-.180	.240
22					-.176	.162
24					-.172	.096
26					-.169	.049
28					-.168	.034
30					-.168	.030
32					-.168	.030
34	1.3000	2.5800	.9600	2.2990	-.118	.080
36	1.1700	1.7850	.9920	2.1840	-.066	.132
38	1.0000	1.0000	1.0000	2.0000	-.008	.190

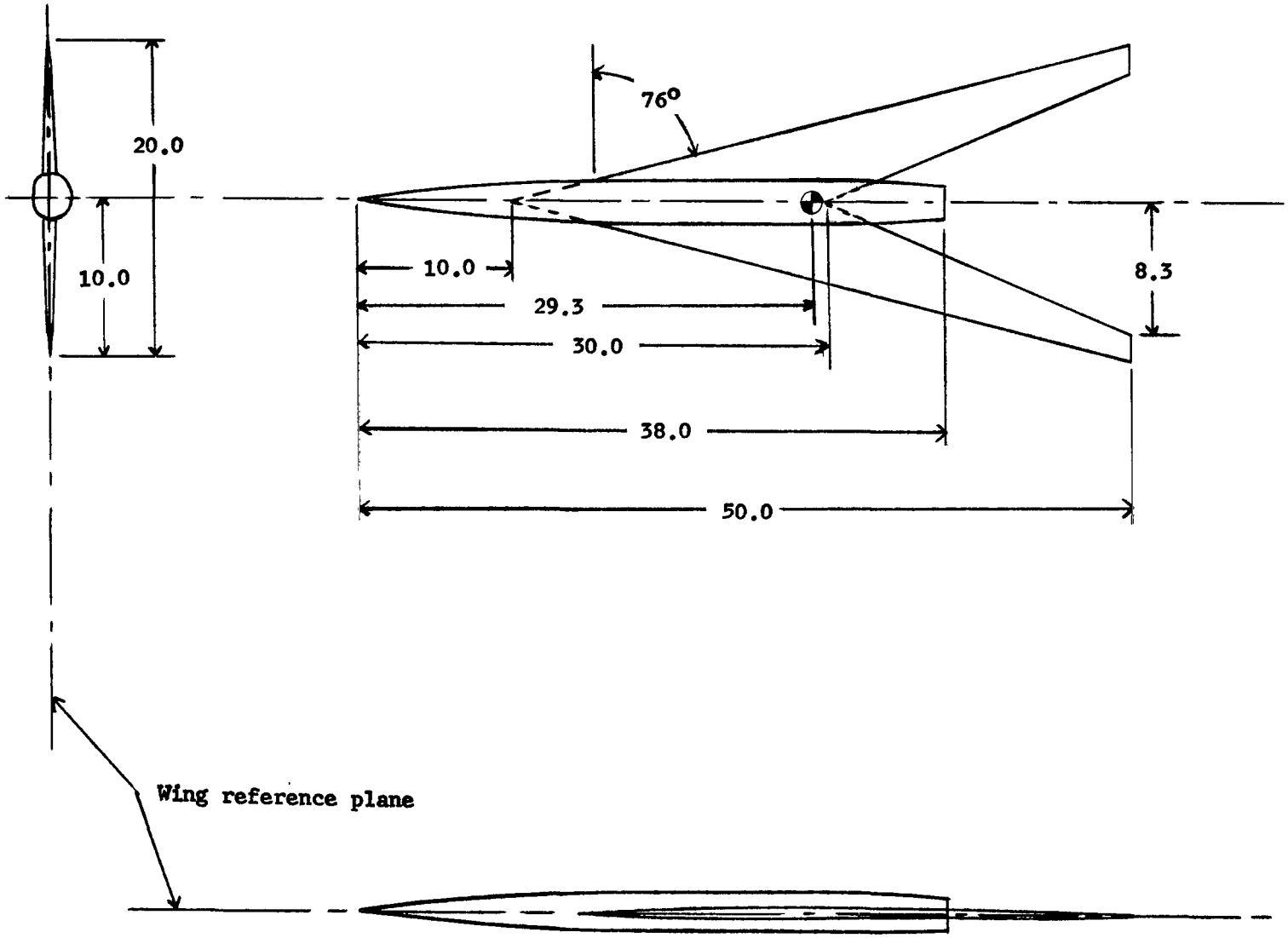

(a) Untwisted and uncambered model; models 1 and 4.

Figure 1.- Three-view drawings representing test configurations. All dimensions are in inches unless otherwise noted.

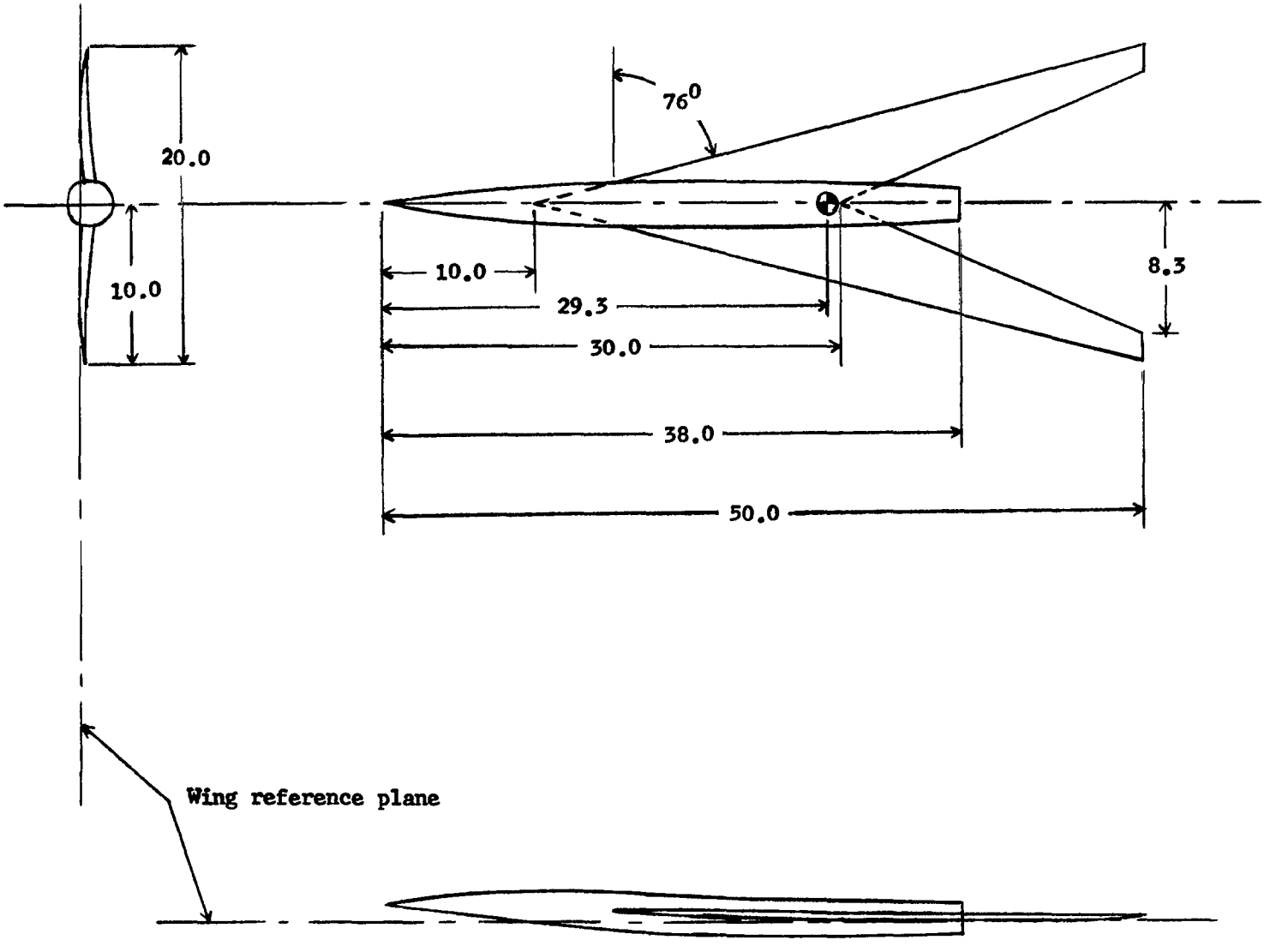

(b) Twisted and cambered model; models 2, 3, and 5.

Figure 1.- Concluded.

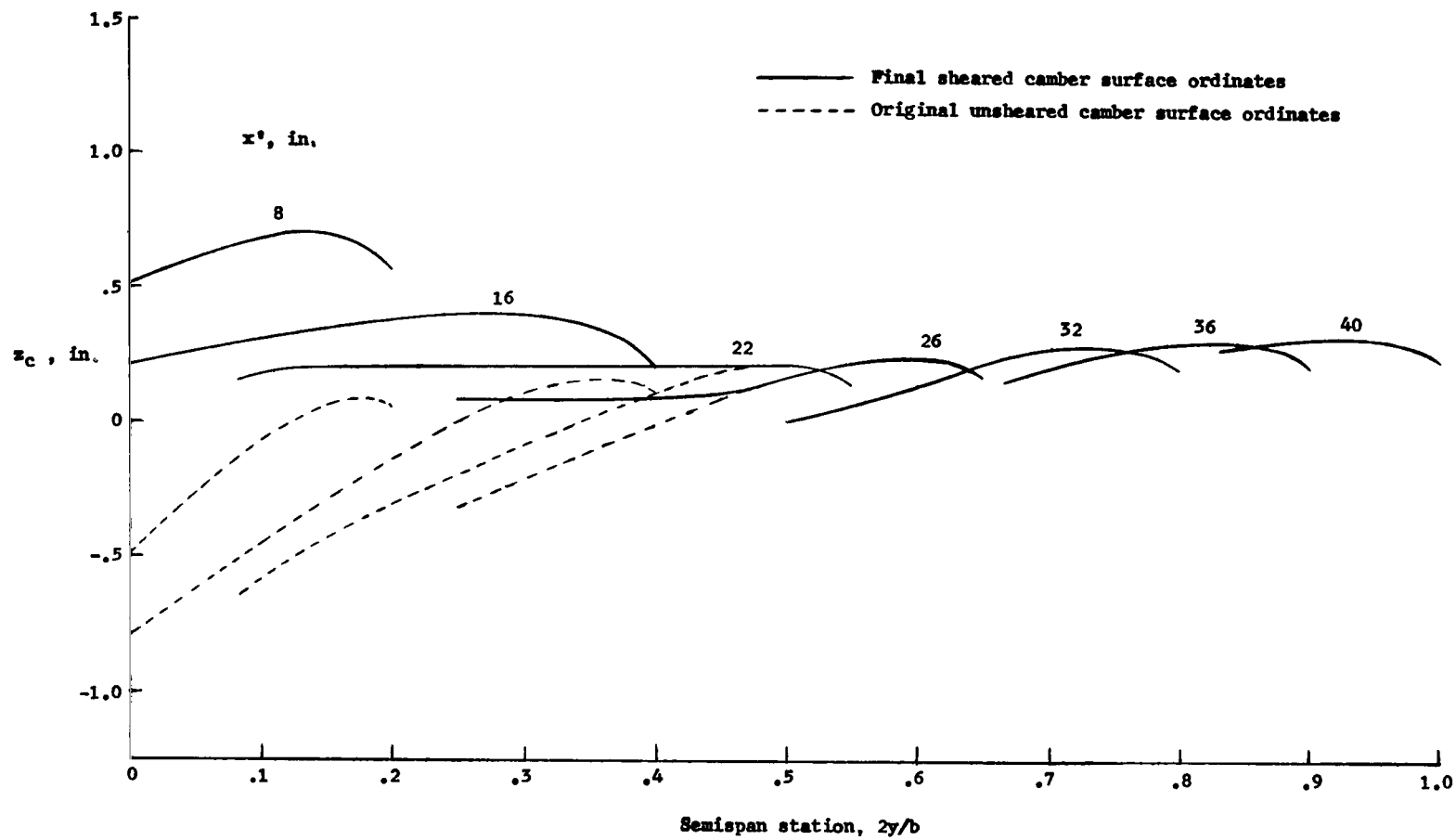

Figure 2.- Original and final camber surface ordinates z_c as a function of semispan station.

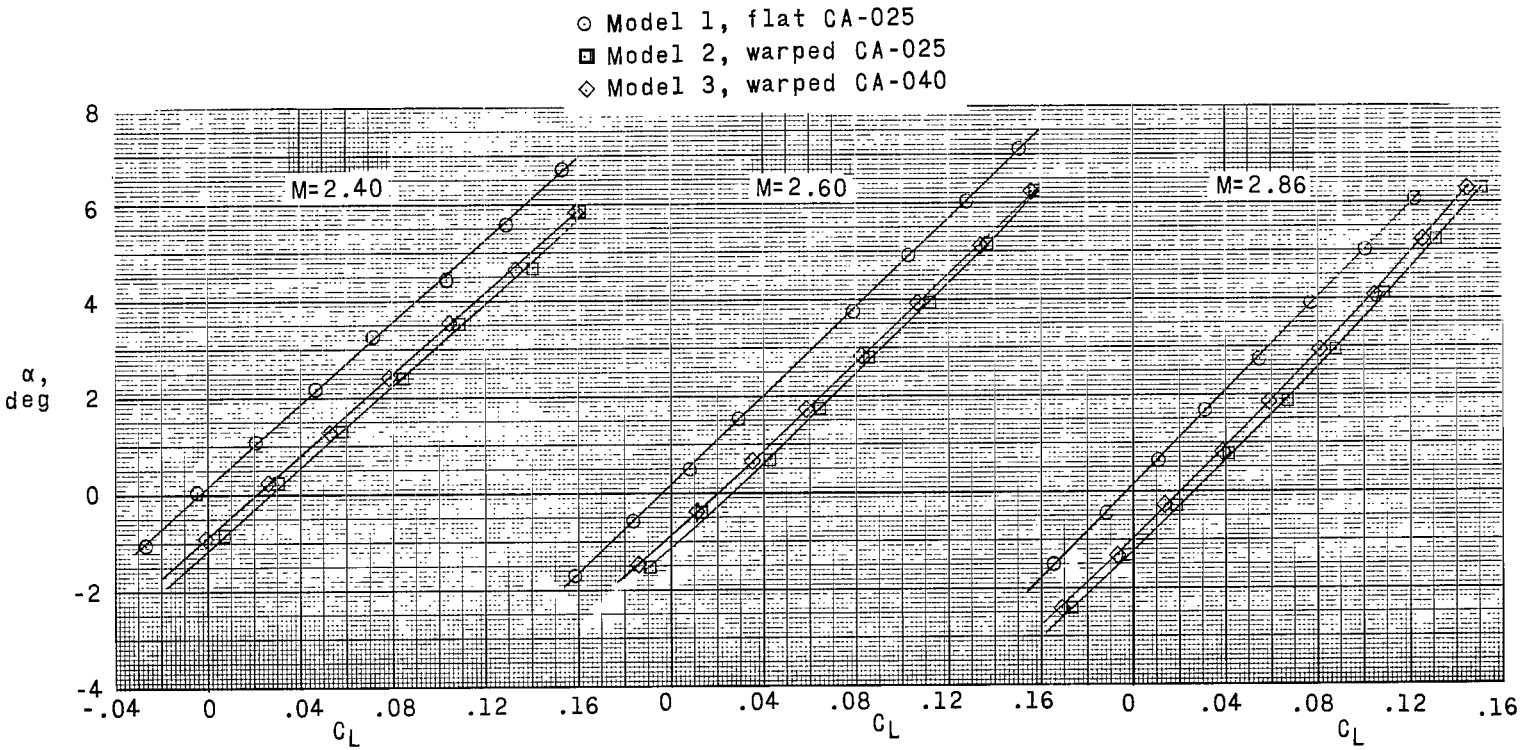

(a) Angle of attack α as a function of lift coefficient C_L.

Figure 3.- Measured aerodynamic characteristics in pitch. Circular-arc thickness distribution.

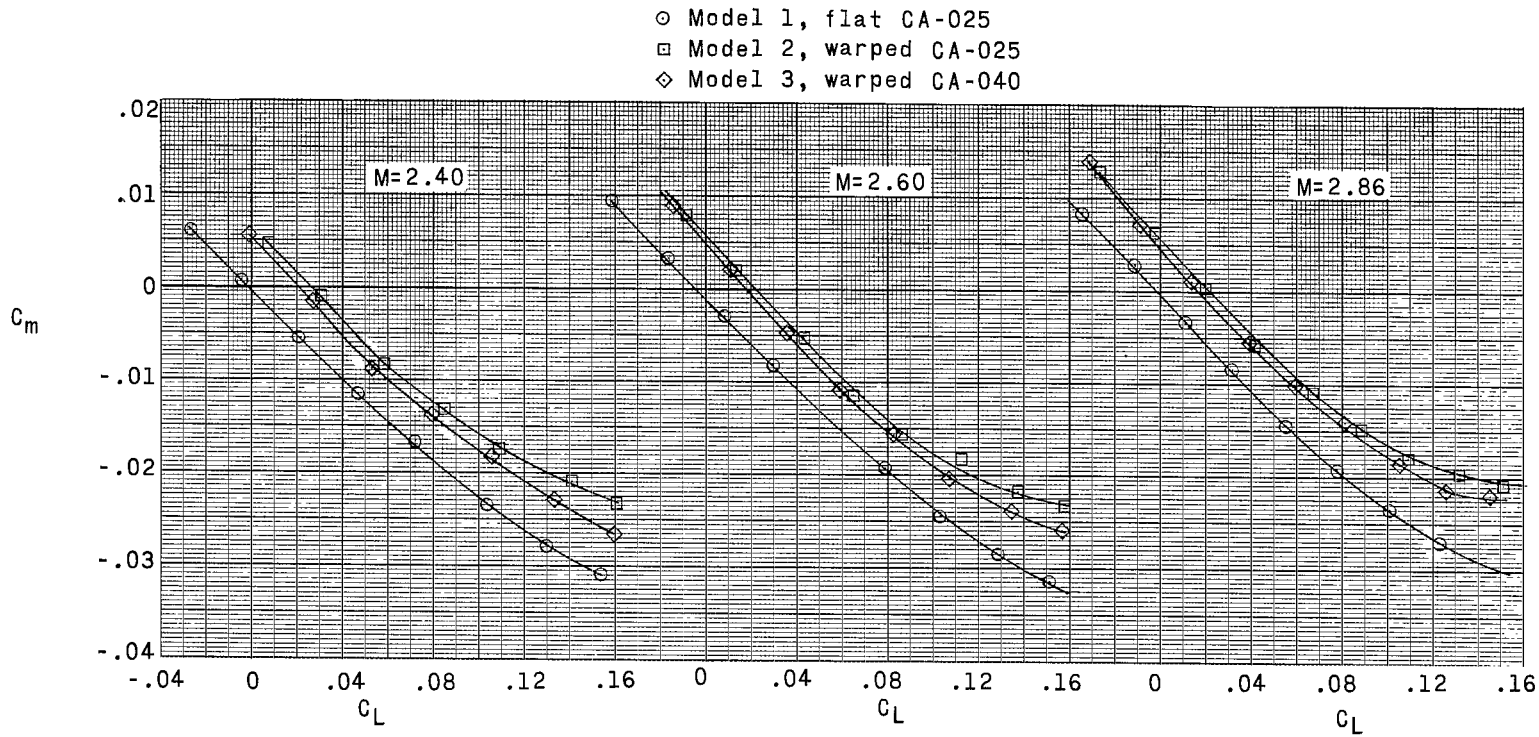

(b) Pitching-moment coefficient C_m as a function of lift coefficient C_L.

Figure 3.- Continued.

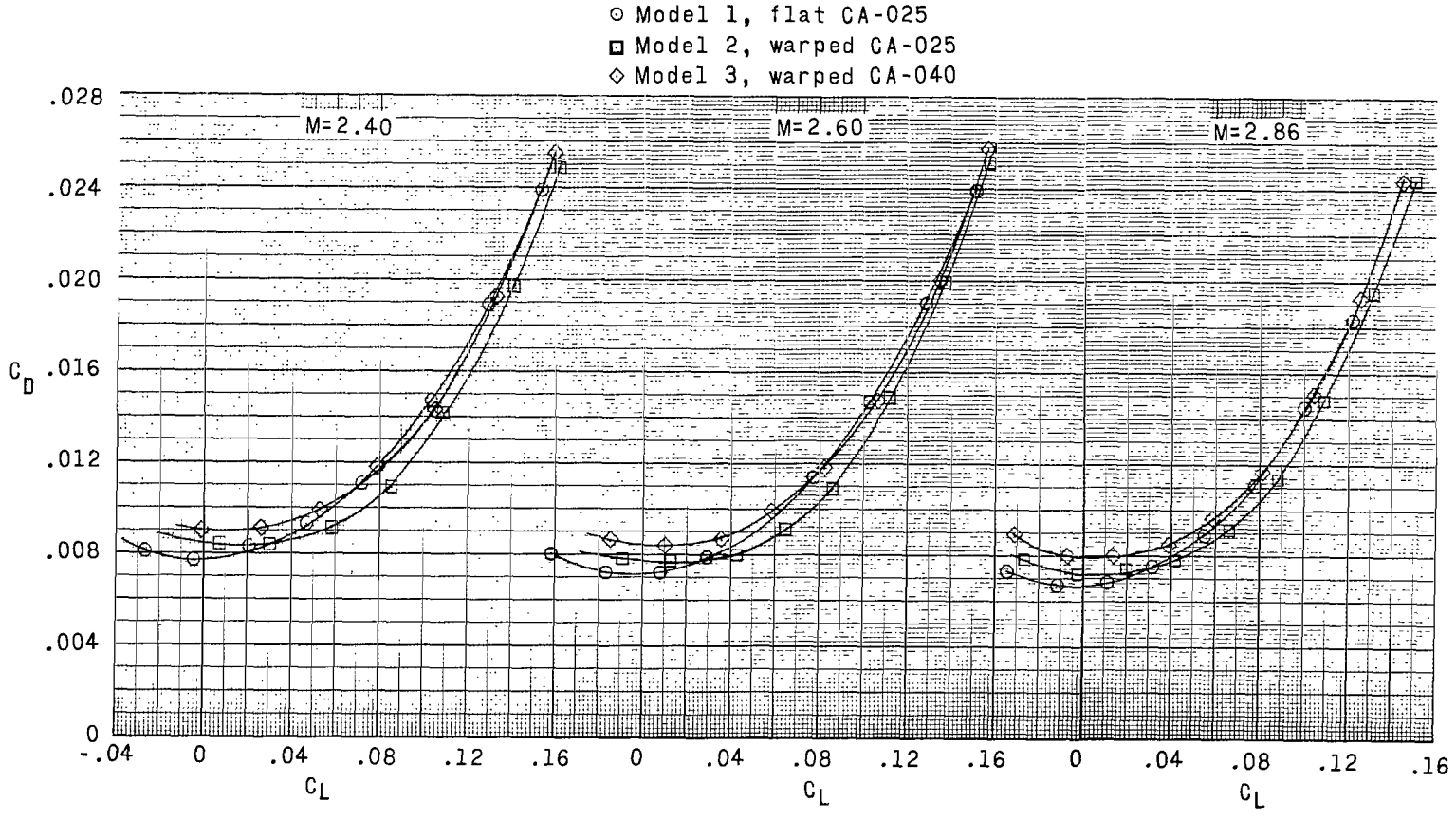

(c) Drag coefficient C_D as a function of lift coefficient C_L.

Figure 3.- Continued.

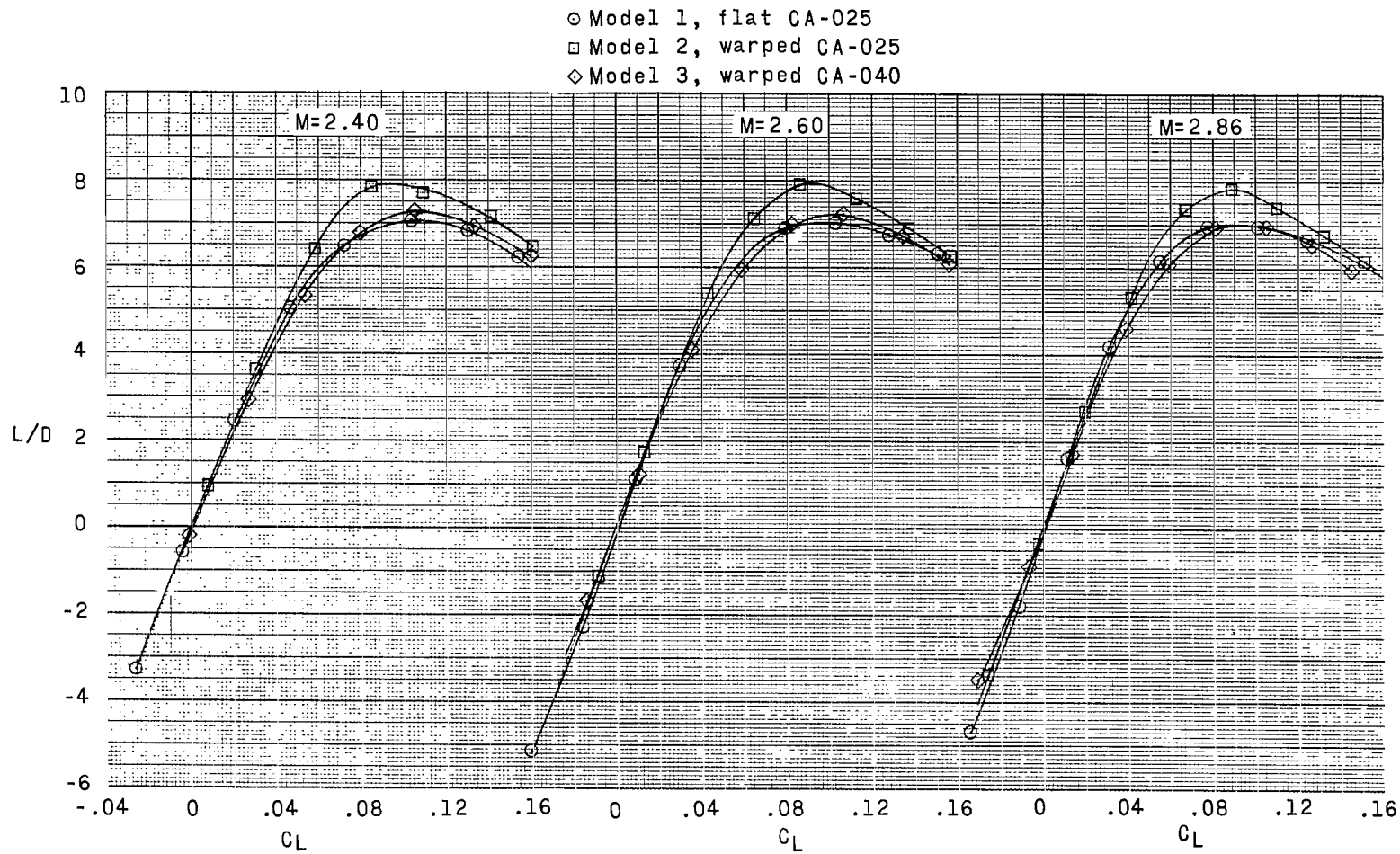

(d) Lift-drag ratio L/D as a function of lift coefficient C_L.

Figure 3.- Concluded.

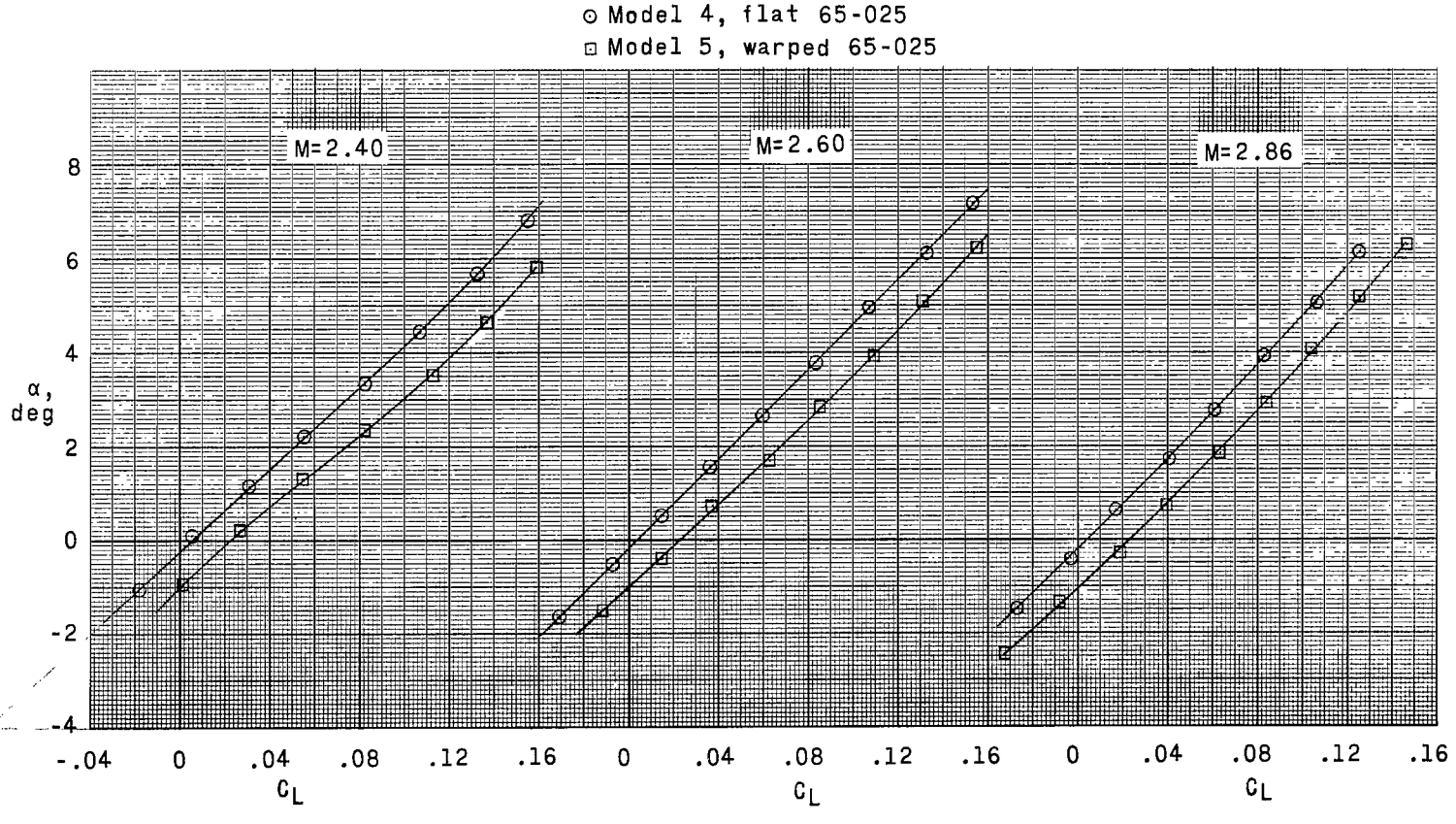

(a) Angle of attack α as a function of lift coefficient C_L.

Figure 4.- Measured aerodynamic characteristics in pitch. 65-series thickness distribution.

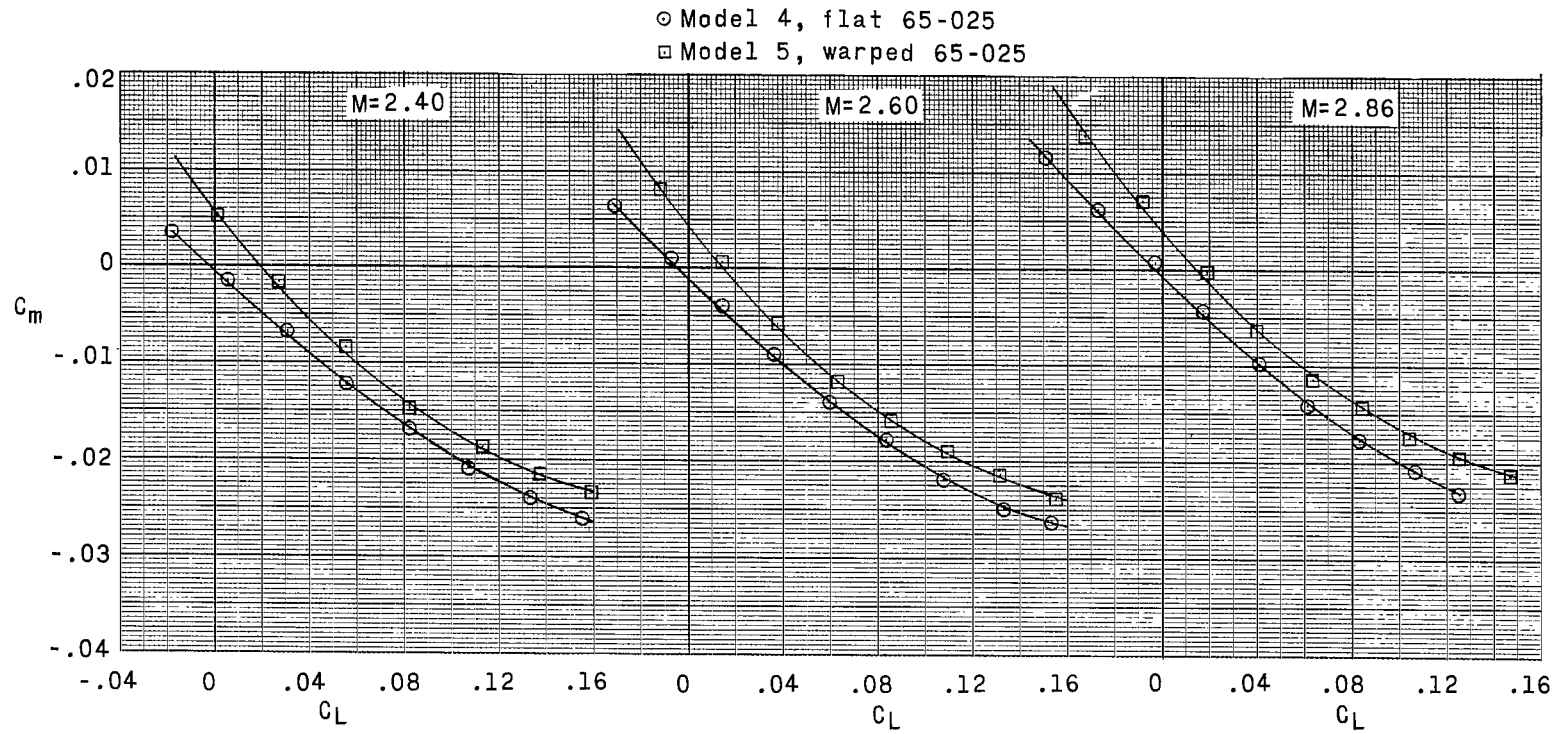

(b) Pitching-moment coefficient C_m as a function of lift coefficient C_L.

Figure 4.- Continued.

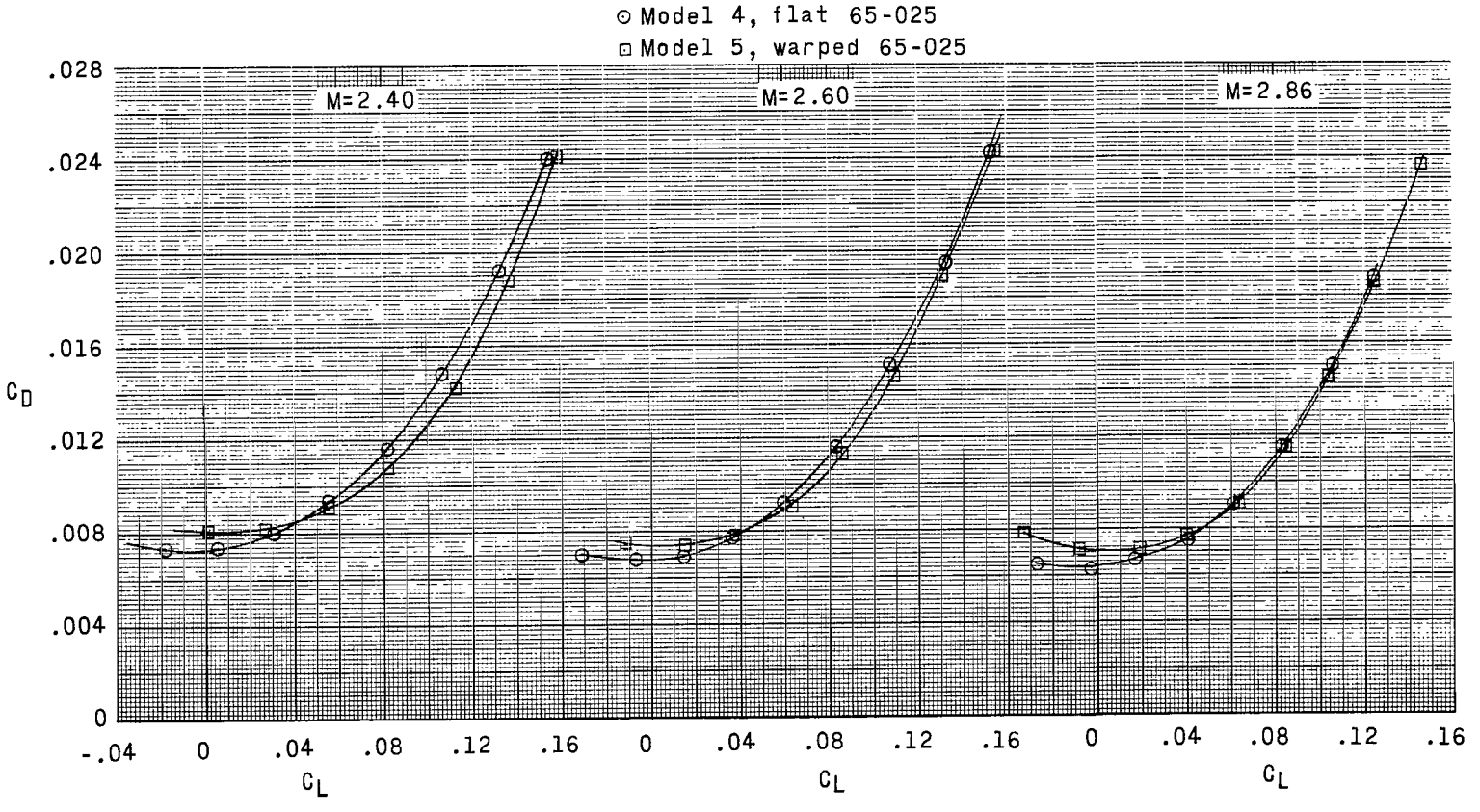

(c) Drag coefficient C_D as a function of lift coefficient C_L.

Figure 4.- Continued.

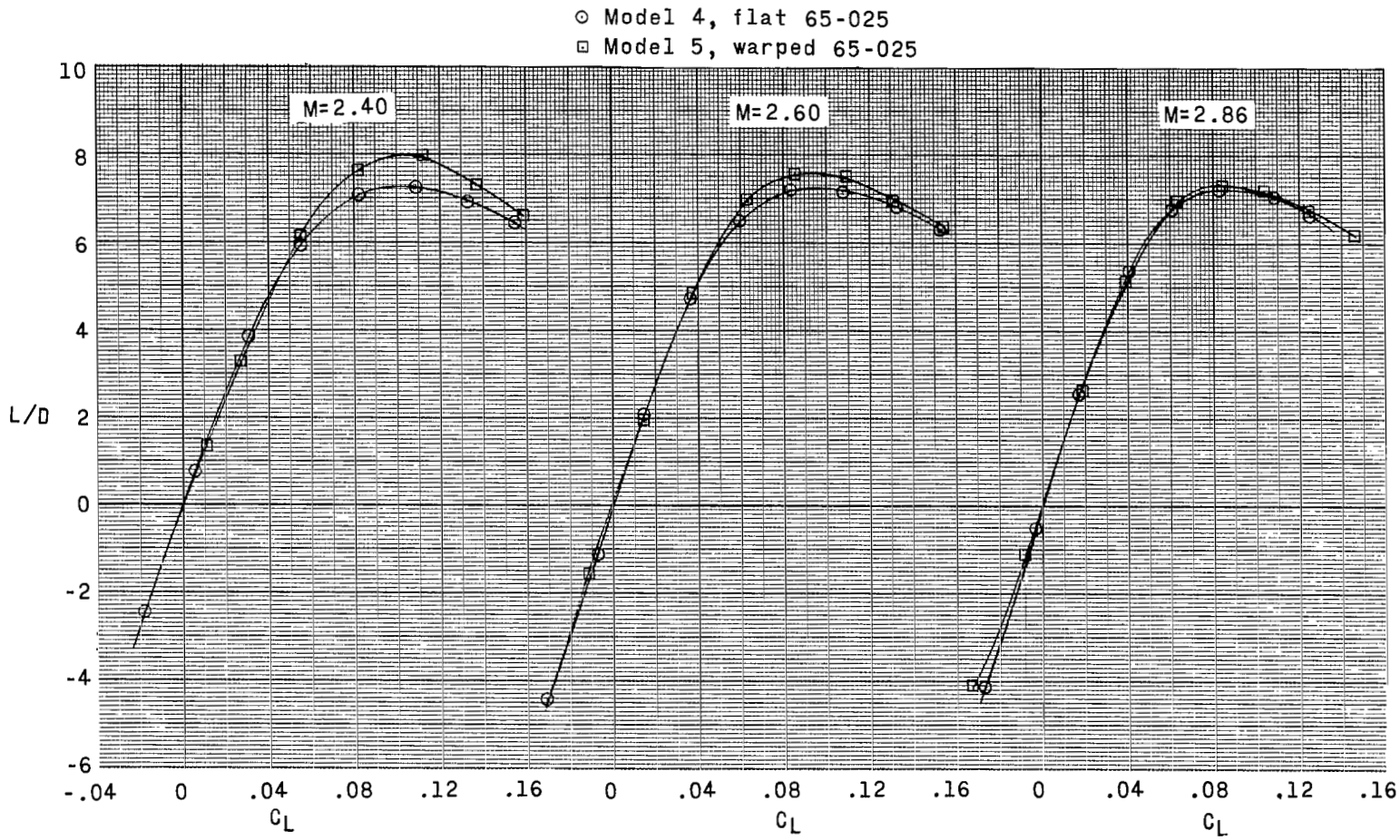

(d) Lift-drag ratio L/D as a function of lift coefficient C_L.

Figure 4.- Concluded.

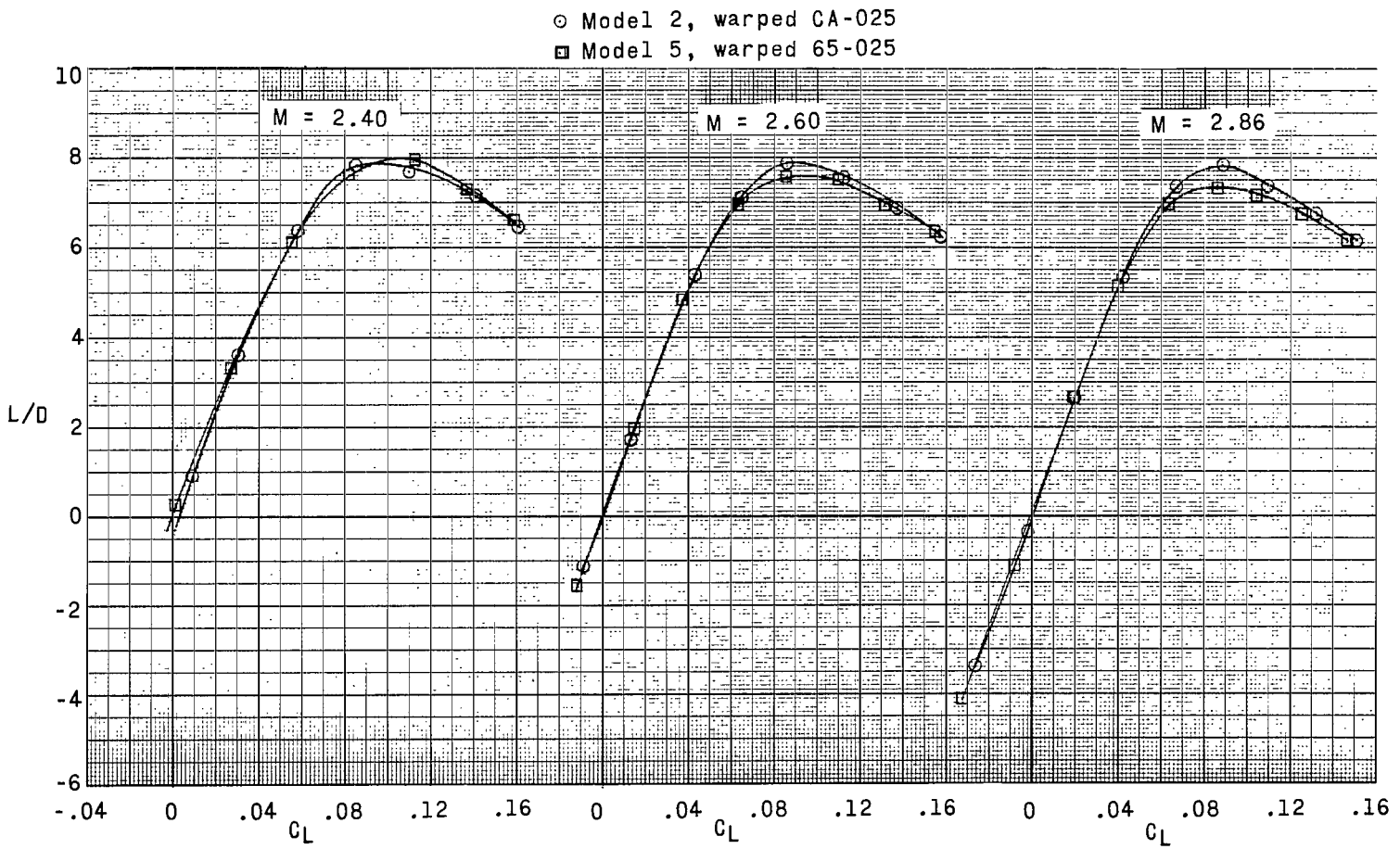

Figure 5.- Effect of airfoil-section shape on the lift-drag ratio of warped configuration.

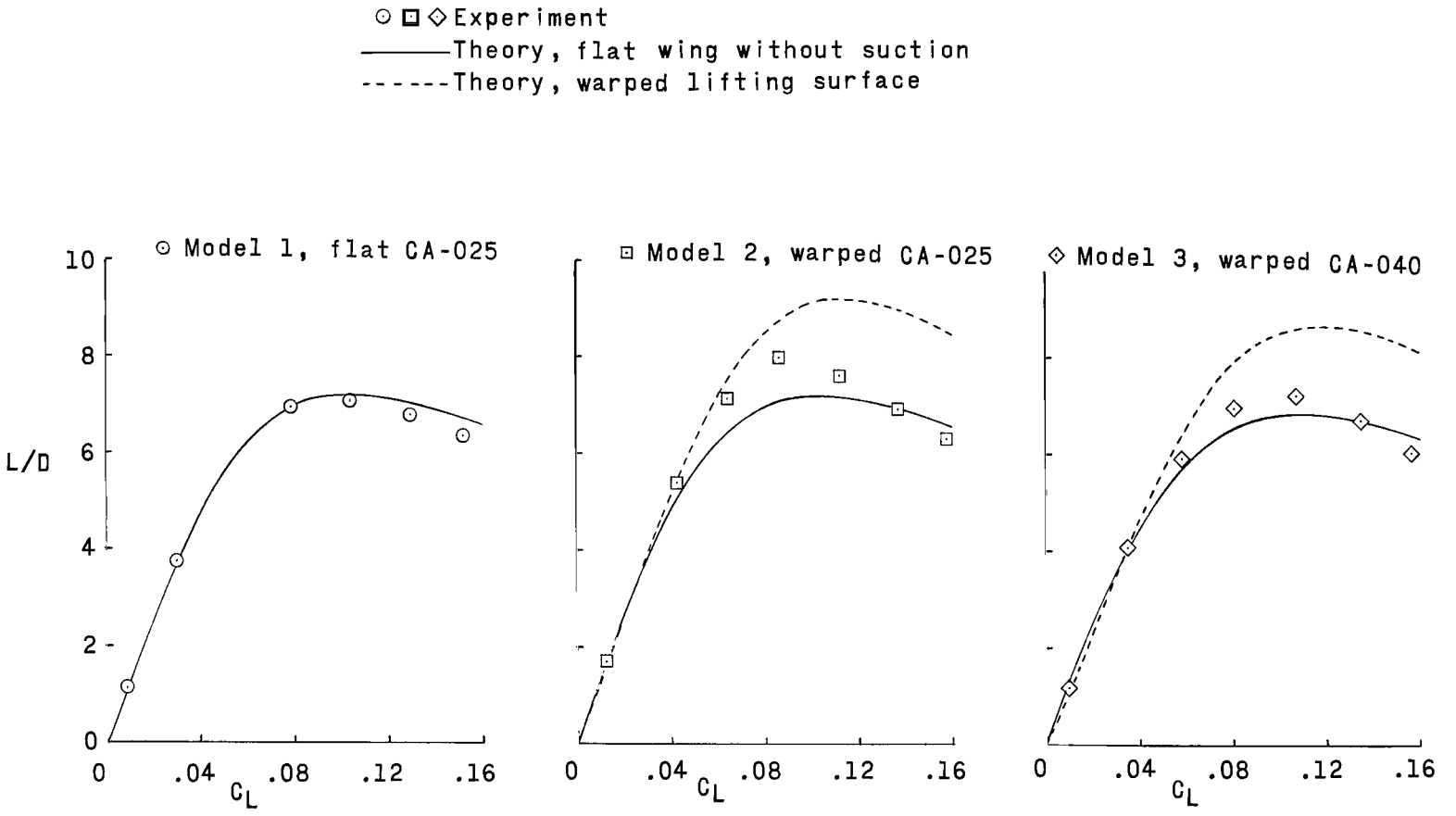

Figure 6.- Comparison of theoretical and experimental lift-drag ratio L/D at M = 2.60. Circular-arc thickness distributions.

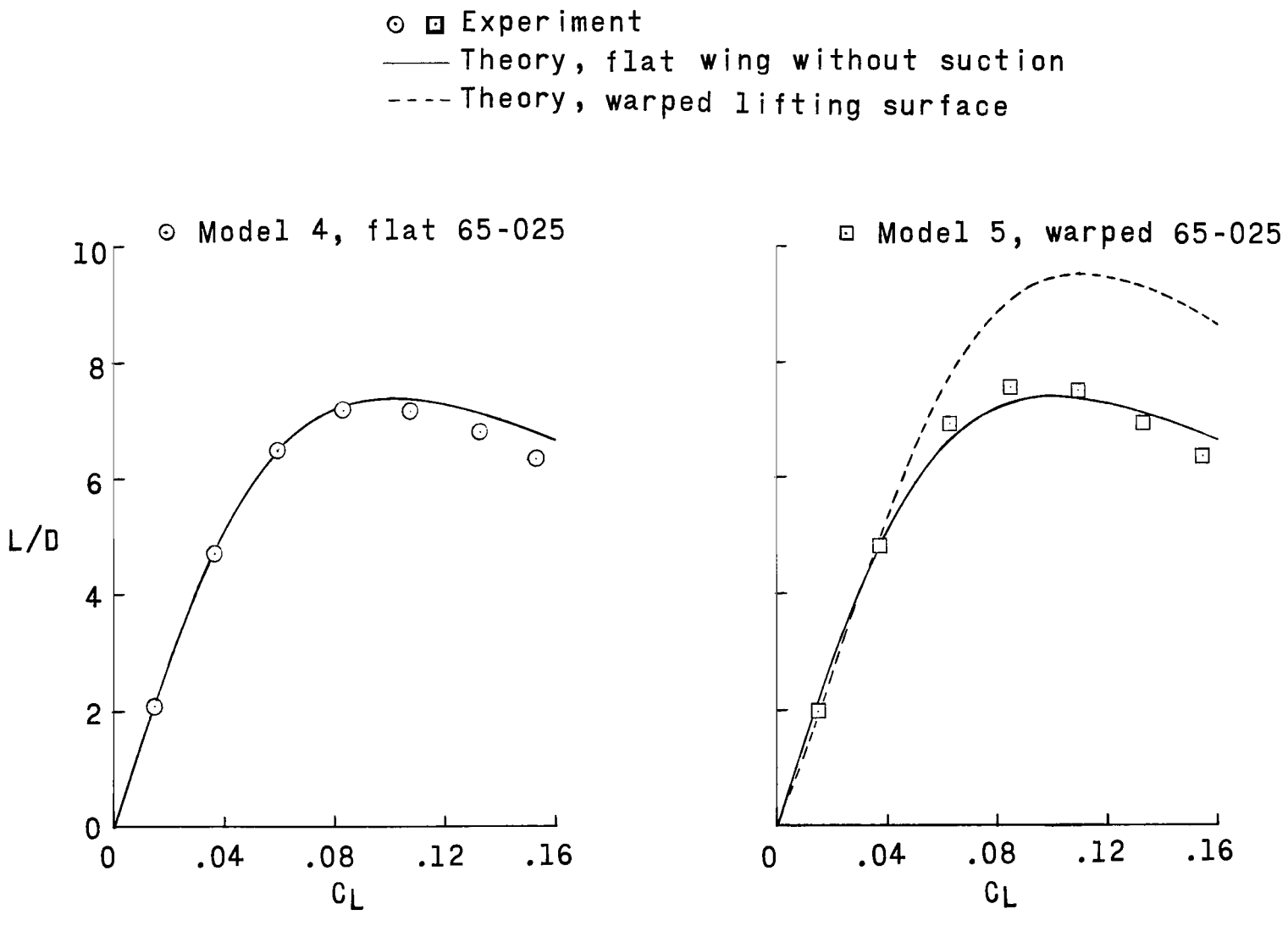

Figure 7.- Comparison of theoretical and experimental lift-drag ratio L/D at M = 2.60. 65-series thickness distributions.

3/18/25
30

"The aeronautical and space activities of the United States shall be conducted so as to contribute . . . to the expansion of human knowledge of phenomena in the atmosphere and space. The Administration shall provide for the widest practicable and appropriate dissemination of information concerning its activities and the results thereof."

—NATIONAL AERONAUTICS AND SPACE ACT OF 1958

NASA SCIENTIFIC AND TECHNICAL PUBLICATIONS

TECHNICAL REPORTS: Scientific and technical information considered important, complete, and a lasting contribution to existing knowledge.

TECHNICAL NOTES: Information less broad in scope but nevertheless of importance as a contribution to existing knowledge.

TECHNICAL MEMORANDUMS: Information receiving limited distribution because of preliminary data, security classification, or other reasons.

CONTRACTOR REPORTS: Technical information generated in connection with a NASA contract or grant and released under NASA auspices.

TECHNICAL TRANSLATIONS: Information published in a foreign language considered to merit NASA distribution in English.

TECHNICAL REPRINTS: Information derived from NASA activities and initially published in the form of journal articles.

SPECIAL PUBLICATIONS: Information derived from or of value to NASA activities but not necessarily reporting the results of individual NASA-programmed scientific efforts. Publications include conference proceedings, monographs, data compilations, handbooks, sourcebooks, and special bibliographies.

Details on the availability of these publications may be obtained from:

SCIENTIFIC AND TECHNICAL INFORMATION DIVISION

NATIONAL AERONAUTICS AND SPACE ADMINISTRATION

Washington, D.C. 20546